

Cover Page



Universiteit Leiden



The handle <http://hdl.handle.net/1887/20273> holds various files of this Leiden University dissertation.

**Author:** Elmalk, Abdalmohsen

**Title:** Exposing biomolecular properties one molecule at a time

**Date:** 2012-12-13

# Chapter 1:

---

*Introduction*

## 1.1 Single molecule detection

In recent years, advances in optical spectroscopy and microscopy have made it possible not only to detect and identify single, freely diffusing or immobilized fluorescent molecules, but also to realize spectroscopic measurements and monitor dynamic molecular processes<sup>(1–10)</sup>. These advances in single-molecule detection at room temperature offer new tools for the study of individual macromolecules and biomolecules in complex condensed matter environments. The investigation of individual molecules one at a time can provide information on the distribution of molecular properties at nanoscale<sup>(11–14)</sup>.

Single molecule detection (SMD) allows real-time observations without the ensemble and time averaging that is present in ensemble methods. In particular, the power of single-molecule measurements lies in the ability to resolve and analyze the properties of sub-populations. Moreover, SMD allows the study of asynchronous or nonsynchronizable reactions, the discovery of short-lived (nanosecond to millisecond lifetimes) transient intermediates, and the observation of process kinetics in full time trajectories. The information content of single molecule fluorescence data can be further increased by monitoring different fluorescence characteristics (e.g. fluorescence intensity, lifetime, emission spectrum). Such measurements allow the probing of reaction kinetics, redox properties, fluorescence enhancement and fluorescence resonant energy transfer for individual macromolecules and biomolecules. Of course, the price to pay for this is that one has to repeat the experiment on large numbers of single molecules to get a statistically significant distribution of results. An exciting aspect of SMD lies in its novelty, which makes it highly likely that many new physical and chemical phenomena are yet to be discovered using this technique.

Few biomolecules, however, are intrinsically fluorescent. To observe them by fluorescence imaging techniques they have to be suitably labeled with fluorescent tags. These labels can either consist of organic dye molecules<sup>(15–19)</sup>, or of natively fluorescent proteins like the green fluorescent protein (GFP) and variants thereof<sup>(20–23)</sup>. A variety of techniques has been developed to achieve specific labeling of the proteins of interest, and to incorporate them in living cells. Constructs using a natively fluorescent protein-tag can be genetically engineered and expressed in live cells.

The development of these single-molecule techniques has opened up new vistas for the study of the functional properties of biological systems. On one hand, it is focused on isolated biomolecules *in vitro*, such as proteins, enzymes, DNA or RNA. On the other hand there is increasing interest in applying these advanced imaging techniques to observe these and other biomolecules in action in their native environment, *i.e.*, the living cell<sup>(3,6,8,22–24)</sup>.

In this thesis we have applied single-molecule techniques to study the photophysics of selected biomolecular systems. The experiments range from a spectroscopic study of a single, supramolecular photosynthetic pigment-protein complex to the detection of enzymatic turn-over of individual redox proteins. The latter case involved the development of novel techniques to monitor redox activity of metalloproteins by means of fluorescence. A brief introduction to the background of this work is given in section 1.4.

## 1.2 Single molecule fluorescence microscopy

Single molecule fluorescence detection offers high specificity and outstanding sensitivity. Because of its sensitivity, fluorescence microscopy has developed into one of the prime methods for single-molecule measurements and fundamental, biomolecular studies<sup>(6,7,19,20,25)</sup>. This development is in large part due to improvements of optical detection schemes based on semiconductor technology which is characterized by a high quantum yield of photon detection (up to 80-90%), an essential prerequisite for observing emission from single molecules<sup>(26)</sup>. On one hand there are the charge-coupled diode-array devices (CCDs)<sup>(26-28)</sup> in which this ultimate level of sensitivity is achieved through suppression of read-out noise and by cooling the detector to reduce thermal shot-noise. They consist of two-dimensional diode arrays that are particularly suitable for full-image acquisition in real time. On the other hand, avalanche photodiodes (APDs)<sup>(26,27,29-31)</sup> have acquired single-photon detectivity by taking advantage of the gain that is associated with the electron-multiplier effect of the near-avalanche mode of operation of a photodiode under reverse bias. An APD is typically a single-point detector, although recently this method of gain by electron multiplication has also been implemented in diode array detectors<sup>(32-34)</sup>.

By incorporating these detectors in suitably designed optical microscopes (Fig. 1A) it becomes possible to spatially resolve and visualize individual, fluorescent molecules. The preferred design of the microscope for single-molecule imaging is the epi-fluorescent mode of operation in which the sample is excited with an appropriate laser source, and the back-scattered fluorescence is detected along the same optical path as the excitation light. Fluorescence, being red-shifted with respect to the absorption spectrum, is separated from the excitation light by a dichroic filter. The spatial resolution is determined by the diffraction-limit, i.e. the numerical aperture (NA) of the objective, and is roughly equal to half the wavelength of fluorescence if  $NA = 1$ <sup>(35)</sup>.

The two different types of detectors, CCDs and APDs, lead to distinctly different types of epi-fluorescence microscopy. A CCD detector allows the real-time visualization of a wide field of view, the size of which is limited by the magnification factor and other geometric

parameters of the imaging optics. Such a detector basically operates as an ultra-sensitive camera. An APD, on the other hand, is the detector of choice for a confocal epi-fluorescent microscope. Here the laser-excited fluorescence that is emitted by the sample in the focus of the objective is refocused onto a pin hole which acts as a spatial filter, after which it is directed to the APD. An image can be reconstructed by monitoring the fluorescence while either scanning the laser focus across the sample using, e.g., a set of movable mirrors, or by spatial translation of the sample using a scanning stage. For the work described in this thesis we have used a wide-field imaging as well as a sample-scanning confocal configuration<sup>(35)</sup>. Both modes of operation were incorporated in one setup, with a sliding mirror assembly to switch from one to the other (figure 1A).

Wide-field excitation combined with epi-fluorescent image detection with a high-sensitive CCD camera has the advantage that large numbers of molecules can be monitored at the same time. The other advantage is the speed of imaging which allows, e.g., the tracking of molecules in space with a time resolution as short as a few milliseconds. It is to be noted that out-of-focus fluorescence from the sample contributes a diffuse background to the image which may reduce the contrast. In the experiments described in Chapter 2 we combined wide-field microscopy (WFM) with wavelength dispersion of the fluorescence to study spectroscopic features of individual pigment-protein complexes. This method is described in more detail in the next section.

In contrast to WFM, scanning confocal microscopy (SCM)<sup>(35)</sup> offers a small detection volume because the pin hole in the detection path only transmits the fluorescence that originates from the laser focus. The size of the pin hole is usually matched to the size of the Airy-disk that is formed by the refocused fluorescence. In that case the transmission of the pin hole and the spatial resolution are optimal. Because the pin hole acts as a spatial filter, a SCM can often provide a much better signal-to-noise ratio than a WFM. A very distinct feature of a SCM is that it can generate a three-dimensional image due to spatially selective fluorescence detection in the lateral as well as the longitudinal direction with respect to the optical axis of the microscope. Because of the intensity profile of the laser excitation beam in the focal region and the confocal optical geometry, the spatial resolution in the lateral scanning directions is higher than in the longitudinal direction<sup>(35)</sup>.

In the work described in this thesis we use the SCM to analyse the photophysical properties of single, fluorescently labeled biomolecules which are immobilized on a chemically modified surface of glass or gold. The purpose of chemical surface modification is to achieve stable adsorption or covalent bonding of the biomolecule to the surface. The experiment typically involves the acquisition of a confocal image after which the coordinates of each fluorescent molecule in the image can be identified and marked. These

molecules are successively targeted by the laser beam to measure the parameters of interest of each molecule, such as the fluorescence spectrum, the fluorescence lifetime, the fluorescence anisotropy and/or the fluorescence time trace (i.e. the photon arrival statistics). The time-resolved experiments require the use of pulsed lasers, but these are readily available with a choice of operating wavelengths to match the absorption spectra of common dye labels and fluorescent proteins. They facilitate the monitoring of temporal processes down to the level of tens of picoseconds. More sophisticated and complex strategies of single-molecule spectroscopy involve multi-color experiments, using more than one excitation laser and/or multiple dye-labels<sup>(36,37)</sup>.

Fluorescence lifetime parameters provide the basis for a quantitative assessment of molecular properties and dynamics. Typical examples are the probing of the local environmental parameters of a fluorophore via lifetime changes, sensing distances on the nanometer scale by Förster resonance energy transfer (FRET), and monitoring functional properties of proteins and enzymes<sup>(2)</sup>.

In the next section we will describe briefly the technical details of the setup that was developed to perform the experiments described in this thesis. It is designed to detect individual fluorescent photons and record their temporal and spectral signature.

### **1.3 Experimental setup**

For the work described in this thesis we have constructed an experimental setup which combined both the wide-field and confocal imaging techniques, see Figure 1A. It incorporates a picosecond red laser (PicoQuant GmbH, LDH-P-639 with PDL 800-B driver) to deliver a continuous train of light pulses at 639 nm for excitation of the sample, with a repetition rate of 40 MHz, and a pulse duration of 90 to 400 ps depending on the setting of the output power. Alternatively, a frequency-doubled, diode-pumped Nd:YAG laser can be used for CW excitation at 532 nm. A polarization-maintaining single-mode fiber guides the laser light to the microscope, with the benefit of a well-defined beam profile from the output end of the fiber. The dichroic mirror (Z 532/633 M, Omega Optical) reflects the light into a high aperture oil immersion objective (Zeiss 100× oil, NA 1.4) which focuses the beam to a diffraction-limited spot (~300 nm diameter) on the sample surface.

In the confocal mode of operation the sample fluorescence is collected through the same objective, transmitted by the dichroic mirror and then filtered by a band pass filter (Omega Optical, D 675/50 M). The fluorescence light is focused by the microscope tube lens into a

50  $\mu\text{m}$  pinhole. An achromatic lens with a focal length of +45 mm refocuses the light onto the active area (175  $\mu\text{m}$  diameter) of a single-photon avalanche diode (APD, Perkin-Elmer SPCM-AQR-14). The data acquisition was done by the TimeHarp 200 TCSPC PC-board working in the special Time-Tagged Time-Resolved Mode, which stores precise timing information of every detected photon for further data analysis. Samples were mounted onto

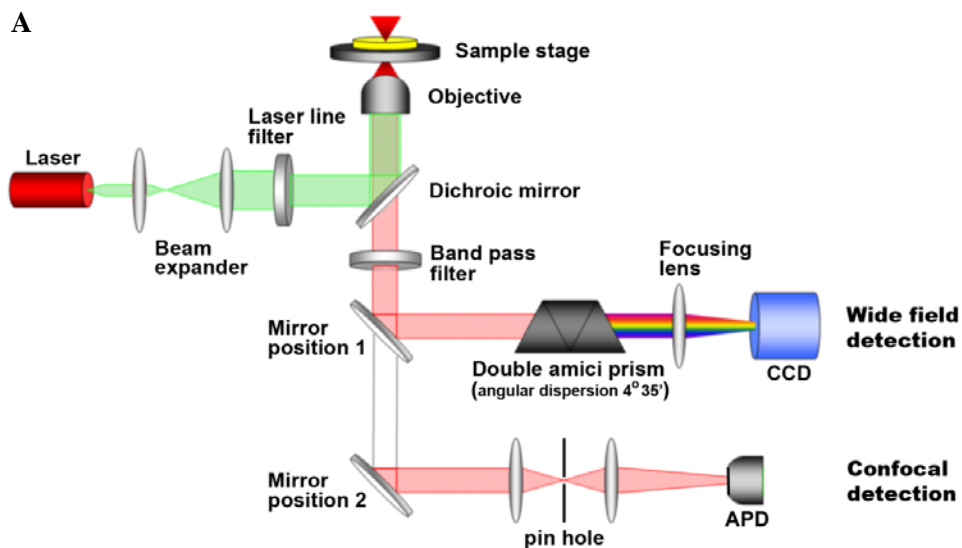
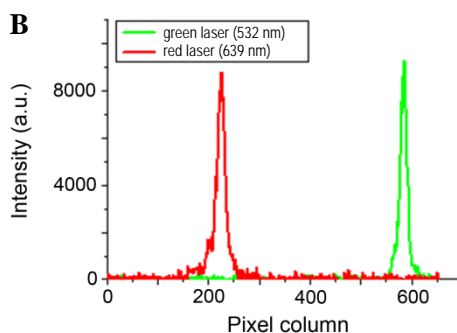


**Figure 1:** The optical setup, based on an Axiovert S100TV inverted microscope, combines a confocal and a wide-field fluorescence microscope. A solid state laser excites fluorescent species of interests. In the confocal detection path, a pinhole rejects the out of focus photons and the fluorescence signal is detected by the avalanche photodiode (APD).

A band pass filter suppresses scattered laser light and selectively transmits the fluorescence. By inserting a mirror in position 1 the setup operates in the wide-field detection mode. In the wide-field path, emitted light is collimated and chromatically dispersed by a double Amici-prism and focused onto a CCD camera. The insert on the right (B) shows the normalized spectral intensity distribution of a green (532 nm) and a red laser (639 nm), emanating from the same optical fiber, dispersed by the double Amici-prism on the CCD detector in wide-field mode. The dispersion is about 0.3 nm/pixel, and the spectral resolution is 1.5 nm.



a P-517 nanopositioner which was equipped with the E710 controller, both from Physik Instrumente GmbH (Germany). Scanning, accurate sample positioning, data collection and analysis were performed by the SymPhoTime software package (PicoQuant GmbH).

The set up can be switched to a wide-field detection scheme by inserting a mirror in the detection path to deflect the (collimated) fluorescence light towards the CCD camera (Cascade 650, Photometrics Inc.). This mode of operation, for example, can be used to locate individual molecules and record their position as a function of time in order to determine diffusion parameters. The experiments described in Chapter 2 of this thesis were designed to determine fluorescence spectra from individual pigment-protein complexes. For this purpose we inserted a double Amici prism (CVI Melles Griot, Inc.) in the optical detection path to spectrally disperse the fluorescence across the CCD array. A schematic diagram of the prism-based wide-field setup is shown in Figure 1 together with the confocal setup.

As mentioned above, a solid state laser (532 nm) or red diode laser (639 nm) was used for the excitation of the sample. An extra lens (not shown) is inserted in the excitation path to achieve wide-field illumination. The fluorescence emission from the sample is collected by the objective and separated from backscattered excitation light with a dichroic mirror (Z532/633M, Omega Optical). An achromatic lens ( $f = 50$  mm) collimates the emission light, which then passes an Amici-prism (PRF-16.4-30-C, CVI Melles Griot, GmbH) dispersing the fluorescence light. Behind the prism, an achromatic focusing lens ( $f = 45$  mm) brings the dispersed fluorescence light into focus for detection with the CCD camera (Cascade 650, Photometrics Inc.).

The system was calibrated by imaging the two laser lines at 532 and 639 nm (Figure 1B), and was found to have an average dispersion of 0.3 nm/pixel and a spectral resolution of about 1.5 nm. The dispersion as a function of wavelength is non-linear, but the wavelength range of interest is in our case (Chapter 2) small enough to assume that the dispersion is more or less constant.

## 1.4 Scope of this thesis

The work described in this thesis was aimed at the study of the functional properties of (isolated and purified) biomolecular systems at the single-molecule level. Two prerequisites are essential for successfully achieving this goal. First of all, single biomolecules should be observable, which means that they should be natively fluorescent or they should be rendered fluorescent by suitable biochemical or biomolecular

engineering. The other challenge is to engineer the system in such a way that the fluorescence intensity reports the actual, functional state of the biomolecule.

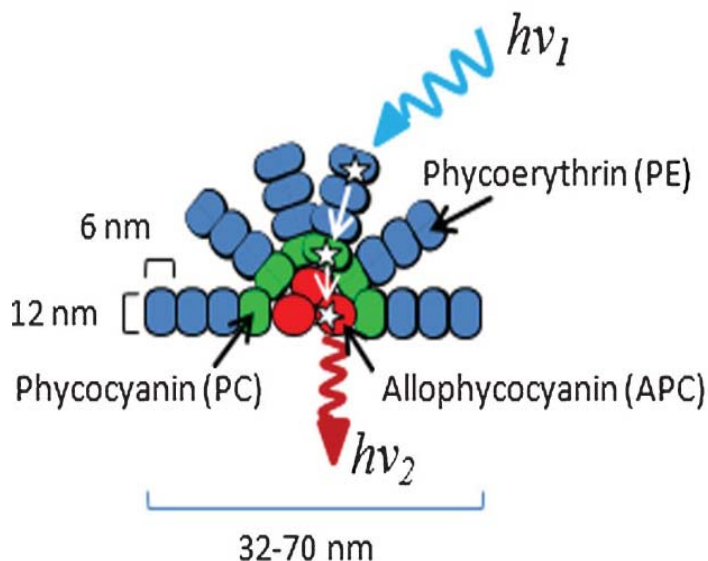


**Figure 2:** Schematic representation of the three main phycobiliprotein groups in the phycobilisome, the light-harvesting antenna complex in cyanobacteria and red algae<sup>(38–41)</sup>. The phycobilisome docks to the membrane-embedded photosynthetic reaction center of the microorganism. The phycobiliproteins, which serve as scaffolding for covalently bound, linear tetrapyrrole chromophores are classified into three types based on their absorption spectra: phycoerythrin (PE), phycocyanin (PC), and allophycocyanin (APC). Hemispherically organized rods of PC and/or PE biliproteins join a core of APC biliproteins. The bulk of the absorption takes place in the rods, while the unique nanostructure facilitates efficient energy transfer towards the core, and from there to the photosynthetic reaction centers.

Phycobiliproteins have strong emission bands that extend well into the red region of the visible spectrum where there is minimal interference from biological materials (e.g. blood, sera and cell culture components). Because of these properties, phycobiliproteins have become promising fluorescent probes for use as a fluorescent marker in immunoassay, flow cytometry, and fluorescence microscopy.

### 1.4.1 Phycobilisomes

Intrinsic fluorescence of amino acid residues like tyrosin and tryptophan in common proteins is not sufficiently bright for achieving single-molecule sensitivity. Other chromophores with sufficiently high fluorescence quantum yields must be present, like in

the fluorescing co-factors in GFP and other natively fluorescent proteins. In chapter 2 of this thesis we describe the study of individual phycobilisomes, brightly fluorescent supramolecular pigment-protein complexes, which have a light-harvesting role in photosynthetic organisms<sup>(38-41)</sup>. The chromophores in these complexes consist of various types of phycobilins. Here we use the fluorescence spectrum, rather than just the intensity, to assess energy transfer and dissipation processes in this system as a function of illumination conditions. Real-time spectral detection at the single-complex level allows us to characterize the dynamic fluorescence behavior of individual phycobilisomes (PBsomes) in response to intense light,

In this work we explored a novel approach to monitor single-molecule fluorescence spectra using a double Amici prism as a dispersion element. It provides the possibility for investigating real-time fluorescent emission dynamics of PBsomes as well as the energy transfer between various PBsome components. It is revealed that green-light-induced photobleaching of a single PBsome consists of an energetic decoupling of phycobilin co-factors within the PBsome rod, serving as a novel pathway of energy dissipation. The results provide insights into the photo-protective roles of PBsomes in red algae in response to excess light energy and the energetic association of pigment-protein complexes.

### **1.4.2 The FluRedox principle**

In the subsequent chapters we focus on the redox activity of metalloproteins, where we take advantage of a new method, the FluRedox principle<sup>(42-49)</sup>, to not only visualize these proteins, but at the same time monitor their redox state in real time at the single-molecule level. Redox reactions drive a plethora of biological and chemical processes ranging from photosynthesis and respiration to industrial catalysis and the operation of fuel cells. The FluRedox methodology opens an entirely new platform for a more detailed study of the dynamics and mechanisms of redox protein activity because of its unsurpassed sensitivity and specificity. The work in this thesis is aimed at the implementation of this novel fluorescence method for single-molecule observation of redox events.

The FluRedox technique makes use of a feature that is characteristic of nearly all redox enzymes and electron transfer proteins, *i.e.*, they possess a redox-active centre with optical characteristics that change markedly when the redox state of the centre changes, that is when the redox center exercises its natural role. The emission intensity of a covalently attached fluorescent label will reflect these absorption changes provided the emission spectrum overlaps with the fluctuating absorption band. The physical mechanism responsible for this phenomenon is known as Förster resonant energy transfer (FRET) and the efficiency depends on the sixth power of the distance between prosthetic group and

label. The only condition for the mechanism to work, therefore, is that the distance between label and prosthetic groups is properly chosen. The change in absorbance modulates the FRET efficiency, hence also the fluorescence intensity of the dye label. Note that usually the redox centers are non-fluorescent, thus FRET then results in quenching of fluorescence.

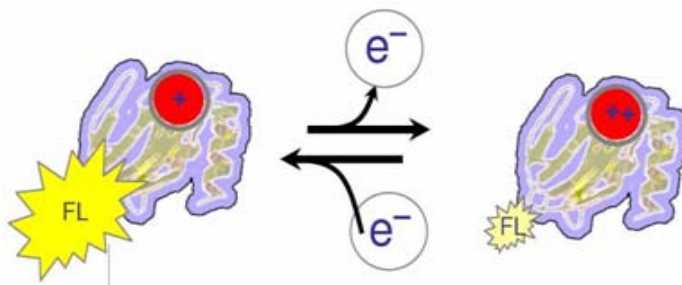


**Figure 3: FluRedox principle**<sup>(42-49)</sup>. The redox protein is linked to a fluorescent dye (FL) which can be excited at a specified wavelength. Subsequently, fluorescence can be measured using a photodiode. The redox state of the protein changes when the active center exchanges electrons either with an electrode or with a reactant in solution. Thus, the change can be translated into the fluorescent intensity of the label covalently attached to the protein surface on the basis of FRET.

Redox proteins and enzymes that contain a so-called Type-1 Cu-atom in their active center are ideal targets for application of the FluRedox technique, as was demonstrated in references<sup>(42-49)</sup>. These blue (Type-1) copper sites are characterised by a strong absorption band at 600 nm when the copper is in the oxidized state<sup>(50)</sup>. This band is absent when the Cu-center is reduced. In this thesis we applied the FluRedox method to azurin and nitrite reductase, both containing a Type-1 Cu center<sup>(51)</sup>. The proteins were labeled with suitable dyes, like Atto-647N or Atto-655, either at the N-terminus or at the -SH group of specifically engineered, surface-exposed cysteines. Turn-over of the redox center of a single molecule through electron exchange with reactants in solution is then observed in real time as step-wise changes of the fluorescence intensity and the fluorescence life time.

### 1.4.3 Fluorescently labeled azurin on a gold surface

Previous work<sup>(46)</sup> has shown that optical tracking of electrochemical events by fluorescence-detected cyclovoltammetry (FCV) already made it possible to determine the electrochemical parameters and redox activity of ensembles of as few as 100 protein molecules. For the combination of fluorescent redox state detection and electronic control the protein together with its fluorescent label needs to be placed close to an electrode, usually a metal surface. This raises questions about the fluorophore-metal interaction, a

subject that has raised considerable interest in recent years from a fundamental as well as an application-oriented perspective. The effect of a metal surface on a nearby fluorophore can lead to both enhancement and quenching of the fluorescence<sup>(52-57)</sup>. Which of these effects dominates is strongly dependent on distance between fluorophore and metal surface. In the work described in this thesis we have elucidated in more detail how the dye-label, when attached to a redox protein, is affected by the interaction with a nearby gold surface. This is important information to further develop the FluRedox method for sensitive electrochemical detection, and to improve our understanding of the recently developed FCV methodology.

We have studied (Chapter 3) the fluorescence of labeled azurin immobilized either on coated glass or on gold films (bare, or coated with a self-assembling monolayer (SAM)) as a function of the thickness of the gold film and the thickness of the SAM. Intensity and lifetime measurements allowed for the separation of enhancement and quenching effects on the fluorescence. In addition, the effect of the redox state on the fluorescence of the labeled protein was investigated. Fluorescence quenching, competing with enhancement, is shown to be a short range effect, and is absent when the SAM is more than 10 carbon atoms high. Significant enhancement is observed with increased roughness of the gold layer.

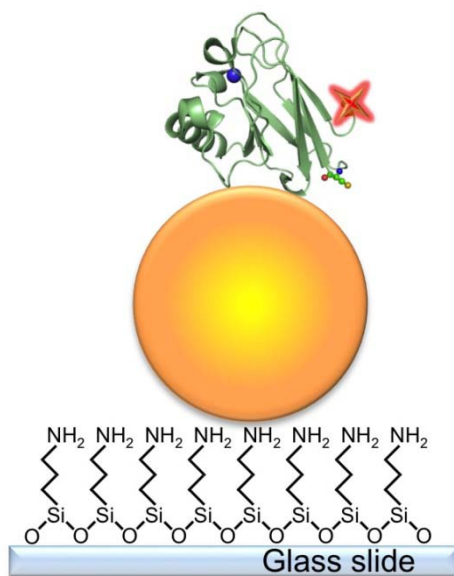
In chapter 4 we focus on the interaction of fluorescently labeled Az with a gold nanoparticle (AuNP). Fluorescence enhancement by NPs and their application in biotechnology is a relatively new subject. A gold NP can function as an optical antenna and through near-field interactions enhance the excitation and fluorescence rate of attached fluorophores. On the other hand, the fluorescence may be *quenched* by energy transfer from the excited fluorophore to the conduction electrons in the NP. Depending on which term is dominant the fluorescence may be enhanced or diminished<sup>(58-63)</sup>. It confronted us with the question how the FluRedox effect would be influenced by a nearby gold NP, and if it could even be enhanced.

To answer this question we have investigated the emission of the fluorescently labeled 14 kDa large copper protein azurin (Az) from *Pseudomonas aeruginosa* immobilized on gold nanoparticles (NPs) as a function of the NP size (1.4-80 nm). Two forms of the Az were studied by single-molecule fluorescence detection: the native form and a form wherein the Cu had been replaced by Zn (ZnAz). Experiments on ZnAz showed that the excitation and radiative rates of the fluorophore were enhanced upon immobilization on AuNPs, but quenching by energy transfer to the NP was observed as well. The results were analyzed quantitatively in terms of a theoretical model which takes into account the influence of the Au NP on the fluorophore excitation rate and quantum yield. Whereas ZnAz is colourless, the native (Cu containing) Az is colourless only in the reduced (Cu<sup>+</sup>) form. It is shown that

attachment of the fluorescently labeled CuAz to a AuNP may lead to a tenfold enhancement of the sensitivity for detecting a redox change of the protein based on the FluRedox principle.

The results illustrate how the redox states of a single protein molecule can be investigated by fluorescence lifetime analysis both for Az on gold and for Az on glass. Thus, the combination of fluorescence lifetime imaging with our FRET-based redox detection method provides a new approach for studying the kinetics of biological electron transfer at the single molecule level. Furthermore, the ability to tune the emission properties of labeled redox proteins immobilized on metal surfaces opens a way to design improved biosensing devices.

**Figure 4:** A schematic representation of Atto647N-labeled azurin adsorbed to AuNPs on a glass slide modified with APTS. The protein framework is depicted in green, the Cu atom in blue and the dye label in red.



#### 1.4.4 Nitrite reductase, one by one.

Single molecule measurements often reveal aspects of protein behavior that are hidden in ensemble measurements. However, applications in enzymology have been limited to enzymes with fluorescent cofactors, substrates or products. One of the main advantages of the FluRedox principle is that it is a platform technology, i.e., it can be applied to any enzyme as long as the prerequisites for FRET with the redox active center can be satisfied. This provides access to a large variety of interesting enzyme systems not only from a scientific point of view, but also for innovative (*e.g.*, biosensor) applications.

In Chapter 5 we successfully demonstrate the potential of the FluRedox principle by the results of single-molecule measurements of the enzymatic activity of nitrite reductase from *Alcaligenes xylosoxidans* (AxNiR). This enzyme converts nitrite into nitric oxide<sup>(64)</sup>. It is a homotrimer, with a binuclear Cu center (T1 and T2). The T1-Cu accepts electrons from a donor and transfers them to the T2-Cu where nitrite is reduced. Oxidized T1-Cu has two broad absorption bands that disappear upon reduction. The FRET efficiency between a fluorescent label and the T1-Cu can be used to follow the catalytic cycle on the basis of fluorescence fluctuations.

For these studies our collaborators at the University of Newcastle (Prof. C. Dennison, D. Kostrz) prepared a mutant of AxNiR with an exposed cysteine (Cys) residue. As AxNiR is a trimer, the Cys in one monomer was used for dye labeling while the Cys in another monomer was used to anchor the enzyme via a molecular linker on a suitably functionalized surface of a microscope cover slip. Fluorescence time-traces of immobilized, single AxNiR in buffer and in the absence of substrates showed typically a steady signal of 2-5 photon counts/ms. The intensity of the signal dramatically increased to

Azurin is a Type 1 blue copper protein with a molecular mass of 14.6 kDa, where the redox-active copper center is either in the 1+ or the 2+ state. Its physiological function has been under debate. Initially it was thought that azurin fulfils a role as electron transporter in the nitrite/nitrate respiratory chain of the microorganism. More recently it was made plausible that the protein has a role in the oxidative stress response<sup>(65)</sup>. A characteristic feature of the Type 1 Cu center is the strong ligand to a cysteine, two imidazoles and two weaker axial ligands, in a distorted trigonal planar geometry.

Copper-containing nitrite reductase (CuNiR) also harbours a Type 1 Cu site bound by two histidines, one cysteine and one methionine<sup>(50)</sup>. In addition, one so-called Type 2 (colourless) copper ion is bound by three histidines. There exists a fourth coordination site for the Cu II centre, which is occupied by water in the resting enzyme and by nitrite in the presence of a substrate. CuNiR enzymes are homotrimers and they can be further classified into blue and green species depending on the details of the ligand geometry of the type 1 Cu sites. They are one of the enzymes that operate in the nitrogen cycle, converting nitrite into nitric oxide.

Azurin and CuNiR are both optically characterized by their intense absorption band in the visible region around 600 nm (azurin) and 430-600 nm (NiR) when the Type 1 copper is oxidized. This band is absent in the reduced state. A state-change can be translated onto the fluorescence intensity of a dye label conjugated to the protein surface using the FluRedox method.

a steady fluorescence rate of 10-30 photon counts/ms by the addition of a reductant (ascorbate/PES), as expected from the reduction of the Type 1 Cu centers. Upon subsequent addition of nitrite the fluorescence time-traces were clearly different. The trace was dominated by a more or less steady 2-5 counts/ms signal with sporadic bursts of 20-30 counts/ms. This behavior can be explained by the T1-Cu fluctuating between the oxidized and reduced state as the enzyme is turning over.

The FRET between dye label and the redox center process not only affects the fluorescence intensity, but also the fluorescence lifetime. This was used to advantage by studying the activity of AxNiR by single-molecule fluorescence lifetime imaging, providing high contrast between the oxidized and reduced form of the enzyme. Immobilized Atto-647N-labeled AxNiR has a lifetime of 3.7 ns in the reduced state, and of 1.1 ns in the oxidized state. By adding a suitable electron donor together with nitrite to the sample, it was possible to observe the catalytic cycling of a single enzyme between the oxidized and reduced forms. Unexpectedly, our studies showed that in turn-over conditions single AxNiR molecules can be sorted in two different populations that follow two different kinetic regimes. Two models have been proposed in the literature for NiR catalysis, a random and a sequential mechanism. Our experiments show that each individual enzyme follows just one of the two possible routes.

## References

1. Schuler B (2007) Application of single molecule Förster resonance energy transfer to protein folding. *Methods in molecular biology* 350:115–38.
2. Joo C, Balci H, Ishitsuka Y, Buranachai C, and Ha T (2008) Advances in single-molecule fluorescence methods for molecular biology. *Annual review of biochemistry* 77:51–76.
3. Xie XS, Choi PJ, Li G-W, Lee NK, and Lia G (2008) Single-molecule approach to molecular biology in living bacterial cells. *Annual review of biophysics* 37:417–44.
4. Kapanidis AN and Strick T (2009) Biology, one molecule at a time. *Trends in biochemical sciences* 34:234–43.
5. Hohlbein J, Gryte K, Heilemann M, and Kapanidis AN (2010) Surfing on a new wave of single-molecule fluorescence methods. *Physical Biology* 7:031001.
6. Lord SJ, Lee HD, and Moerner WE (2010) Single-molecule spectroscopy and imaging of biomolecules in living cells. *Analytical chemistry* 82:2192–203.
7. Toomre D and Bewersdorf J (2010) A new wave of cellular imaging. *Annual review of cell and developmental biology* 26:285–314.

8. Yang H (2010) Progress in single-molecule spectroscopy in cells. *Current opinion in chemical biology* 14:3–9.
9. Fitzpatrick JAJ and Lillemeier BF (2011) Fluorescence correlation spectroscopy: linking molecular dynamics to biological function in vitro and in situ. *Current opinion in structural biology* 21:650–60.
10. Schäfer R and Schmidt PC, ed. (2012) *Methods in Physical Chemistry*. Weinheim, Germany: Wiley-VCH Verlag GmbH & Co. KGaA.
11. Barkai E, Jung Y, and Silbey R (2004) Theory of single-molecule spectroscopy: beyond the ensemble average. *Annual review of physical chemistry* 55:457–507.
12. Gopich IV and Szabo A (2006) Theory of the statistics of kinetic transitions with application to single-molecule enzyme catalysis. *The Journal of chemical physics* 124:154712.
13. Watkins LP and Yang H (2005) Detection of intensity change points in time-resolved single-molecule measurements. *The journal of physical chemistry. B* 109:617–28.
14. Yang H (2008) Model-Free Statistical Reduction of Single-Molecule Time Series. ... *and Evaluation of Single-Molecule Signals edited by E ...*:1–29.
15. Buschmann V, Weston KD, and Sauer M (2002) Spectroscopic study and evaluation of red-absorbing fluorescent dyes. *Bioconjugate chemistry* 14:195–204. American Chemical Society.
16. Resch-Genger U, Grabolle M, Cavaliere-Jaricot S, Nitschke R, and Nann T (2008) Quantum dots versus organic dyes as fluorescent labels. *Nature methods* 5:763–75. Nature Publishing Group.
17. Berezin MY and Achilefu S (2010) Fluorescence lifetime measurements and biological imaging. *Chemical reviews* 110:2641–84. American Chemical Society.
18. Gonçalves MST (2009) Fluorescent labeling of biomolecules with organic probes. *Chemical reviews* 109:190–212. American Chemical Society.
19. Bunt G (2011) Optical Fluorescence Microscopy. In *Optical Fluorescence Microscopy*, ed. A Diaspro, pp. 111–130. Berlin, Heidelberg: Springer Berlin Heidelberg.
20. Chudakov DM, Lukyanov S, and Lukyanov KA (2005) Fluorescent proteins as a toolkit for in vivo imaging. *Trends in biotechnology* 23:605–13.
21. Shaner NC, Steinbach PA, and Tsien RY (2005) A guide to choosing fluorescent proteins. *Nature methods* 2:905–9.
22. Müller-Taubenberger A and Anderson KI (2007) Recent advances using green and red fluorescent protein variants. *Applied microbiology and biotechnology* 77:1–12.
23. Chudakov DM, Matz MV, Lukyanov S, and Lukyanov KA (2010) Fluorescent proteins and their applications in imaging living cells and tissues. *Physiological reviews* 90:1103–63.
24. Patterson G, Davidson M, Manley S, and Lippincott-Schwartz J (2010) Superresolution imaging using single-molecule localization. *Annual review of physical chemistry* 61:345–67. Annual Reviews.
25. Wu B, Piatkevich KD, Lionnet T, Singer RH, and Verkhusha VV (2011) Modern fluorescent proteins and imaging technologies to study gene expression, nuclear localization, and dynamics. *Current opinion in cell biology* 23:310–7.

26. Michalet X, Sigmund OHW, Vallerga JV, Jelinsky P, Millaud JE, and Weiss S (2007) Detectors for single-molecule fluorescence imaging and spectroscopy. *Journal of modern optics* 54:239. Taylor & Francis.
27. Moerner WE and Fromm DP (2003) Methods of single-molecule fluorescence spectroscopy and microscopy. *Review of Scientific Instruments* 74:3597.
28. Rizzuto R, Carrington W, and Tuft RA (1998) Digital imaging microscopy of living cells. *Trends in cell biology* 8:288–92.
29. Cova S, Ghioni M, Lacaita A, Samori C, and Zappa F (1996) Avalanche photodiodes and quenching circuits for single-photon detection. *Applied Optics* 35:1956. OSA.
30. Zappa F (1996) Solid-state single-photon detectors. *Optical Engineering* 35:938.
31. Renker D and Lorenz E (2009) Advances in solid state photon detectors. *Journal of Instrumentation* 4:P04004–P04004.
32. Michalet X, Colyer RA, Scalia G, Kim T, Levi M, Aharoni D, Cheng A, et al. (2010) High-throughput single-molecule fluorescence spectroscopy using parallel detection. *Proceedings - Society of Photo-Optical Instrumentation Engineers* 7608:76082D–76082D–12.
33. Colyer RA, Scalia G, Villa FA, Guerrieri F, Tisa S, Zappa F, Cova S, Weiss S, and Michalet X (2011) Ultra high-throughput single molecule spectroscopy with a 1024 pixel SPAD. In *SPIE BiOS*, pp. 790503–790503–8.
34. Privitera S, Tudisco S, Lanzanò L, Musumeci F, Pluchino A, Scordino A, Campisi A, et al. (2008) Single Photon Avalanche Diodes: Towards the Large Bidimensional Arrays. *Sensors* 8:4636–4655. Molecular Diversity Preservation International.
35. Webb RH (1996) Confocal optical microscopy. *Reports on Progress in Physics* 59:427–471.
36. Cagnet L, Harms GS, Blab GA, Lommerse PHM, and Schmidt T (2000) Simultaneous dual-color and dual-polarization imaging of single molecules. *Applied Physics Letters* 77:4052.
37. Kapanidis A and Laurence T (2005) Alternating-laser excitation of single molecules. *Accounts of chemical research* 38:523–533.
38. Glazer AN (1994) Phycobiliproteins — a family of valuable, widely used fluorophores. *Journal of Applied Phycology* 6:105–112.
39. MacColl R (1998) Cyanobacterial phycobilisomes. *Journal of structural biology* 124:311–34.
40. Ducret A, Sidler W, Wehrli E, Frank G, and Zuber H (1996) Isolation, Characterization and Electron Microscopy Analysis of A Hemidiscoidal Phycobilisome Type from the Cyanobacterium *Anabaena* sp. PCC 7120. *European Journal of Biochemistry* 236:1010–1024.
41. Adir N (2005) Elucidation of the molecular structures of components of the phycobilisome: reconstructing a giant. *Photosynthesis research* 85:15–32.
42. Schmauder R, Librizzi F, Canters GW, Schmidt T, and Aartsma TJ (2005) The oxidation state of a protein observed molecule-by-molecule. *ChemPhysChem* 6:1381–6.
43. Kuznetsova S, Zauner G, Schmauder R, Mayboroda O a, Deelder AM, Aartsma TJ, and Canters GW (2006) A Förster-resonance-energy transfer-based method for fluorescence detection of the protein redox state. *Analytical biochemistry* 350:52–60.

44. Zauner G, Lonardi E, Bubacco L, Aartsma TJ, Canters GW, and Tepper AWJW (2007) Tryptophan-to-dye fluorescence energy transfer applied to oxygen sensing by using type-3 copper proteins. *Chemistry Eur J* 13:7085–90.
45. Davis JJ, Burgess H, Zauner G, Kuznetsova S, Salverda J, Aartsma T, and Canters GW (2006) Monitoring interfacial bioelectrochemistry using a FRET switch. *The journal of physical chemistry. B* 110:20649–54.
46. Salverda JM, Patil AV, Mizzon G, Kuznetsova S, Zauner G, Akkilic N, Canters GW, Davis JJ, Heering HA, and Aartsma TJ (2010) Fluorescent Cyclic Voltammetry of Immobilized Azurin: Direct Observation of Thermodynamic and Kinetic Heterogeneity. *Angewandte Chemie (Intern. Ed.)* 122:5912–5915.
47. Goldsmith RH, Tabares LC, Kostrz D, Dennison C, Aartsma TJ, Canters GW, and Moerner WE (2011) Redox cycling and kinetic analysis of single molecules of solution-phase nitrite reductase. *Proceedings of the National Academy of Sciences of the United States of America* 108:17269–74.
48. Kuznetsova S, Zauner G, Aartsma TJ, Engelkamp H, Hatzakis N, Rowan AE, Nolte RJM, Christianen PCM, and Canters GW (2008) The enzyme mechanism of nitrite reductase studied at single-molecule level. *Proceedings of the National Academy of Sciences of the United States of America* 105:3250–5.
49. Gustiananda M, Andreoni A, Tabares LC, Tepper AWJW, Fortunato L, Aartsma TJ, and Canters GW (2011) Sensitive detection of histamine using fluorescently labeled oxido-reductases. *Biosensors and Bioelectronics*: Elsevier B.V.
50. Adman ET (1991) Structure and function of copper-containing proteins. *Current Opinion in Structural Biology* 1:895–904.
51. Jeuken LJC, Vliet PV, Verbeet MP, Camba R, Mcevoy JP, Armstrong FA, and Canters GW (2000) Role of the Surface-Exposed and Copper-Coordinating Histidine in Blue Copper Proteins: The Electron-Transfer and Redox-Coupled Ligand Binding Properties of His117Gly Azurin. *Journal of the American Chemical Society* 122:12186–12194.
52. Prigogine I and Rice SA, ed. (1978) *Advances in Chemical Physics*. Hoboken, NJ, USA: John Wiley & Sons, Inc.
53. Drexhage KH (1970) Influence of a dielectric interface on fluorescence decay time. *Journal of Luminescence* 1-2:693–701.
54. Hellen EH and Axelrod D (1987) Fluorescence emission at dielectric and metal-film interfaces. *Journal of the Optical Society of America B* 4:337. OSA.
55. Fort E and Grésillon S (2008) Surface enhanced fluorescence. *Journal of Physics D: Applied Physics* 41:013001.
56. Lakowicz JR (2005) Radiative decay engineering 5: metal-enhanced fluorescence and plasmon emission. *Analytical biochemistry* 337:171–94.
57. Waldeck DH, Alivisatos AP, and Harris CB (1985) Nonradiative damping of molecular electronic excited states by metal surfaces. *Surface Science* 158:103–125.
58. Härtling T, Reichenbach P, and Eng LM (2007) Near-field coupling of a single fluorescent molecule and a spherical gold nanoparticle. *Optics Express* 15:12806. OSA.

59. Kühn S, Håkanson U, Rogobete L, and Sandoghdar V (2006) Enhancement of Single-Molecule Fluorescence Using a Gold Nanoparticle as an Optical Nanoantenna. *Physical Review Letters* 97:017402.
60. Bharadwaj P, Anger P, and Novotny L (2007) Nanoplasmonic enhancement of single-molecule fluorescence. *Nanotechnology* 18:044017.
61. Taminiau TH, Stefani FD, Segerink FB, and van Hulst NF (2008) Optical antennas direct single-molecule emission. *Nature Photonics* 2:234–237.
62. Lakowicz JR and Fu Y (2009) Modification of single molecule fluorescence near metallic nanostructures. *Laser & Photonics Review* 3:221–232.
63. Anger P, Bharadwaj P, and Novotny L (2006) Enhancement and Quenching of Single-Molecule Fluorescence. *Physical Review Letters* 96:113002.
64. Adman E and Murphy M (2001) Copper Nitrite Reductase. In *Encyclopedia of Inorganic and Bioinorganic Chemistry*, ed. RA Scott. Chichester, UK: John Wiley & Sons, Ltd.
65. Vijgenboom E, Busch JE, and Canters GW (1997) In vivo studies disprove an obligatory role of azurin in denitrification in *Pseudomonas aeruginosa* and show that *azu* expression is under control of *rpoS* and *ANR*. *Microbiology* 143:2853–63.